

THE FLUKA RADIATION TRANSPORT CODE AND ITS USE FOR SPACE PROBLEMS

Alfredo Ferrari[#], Johannes Ranft* and Paola R. Sala[#]

[#] CERN, 1211 Geneva 23, Switzerland

(on leave of absence from INFN Milan)

* Phys. Dept., Universität Siegen, D-57068 Siegen, Germany

Keynote lecture presented at the

*1st International Workshop on Space Radiation Research
and
11th Annual NASA Space Radiation Health Investigators'
Workshop*

Arona, Italy, 27 -31 may 2000

Proceedings in press

THE FLUKA RADIATION TRANSPORT CODE AND ITS USE FOR SPACE PROBLEMS

Alfredo Ferrari[#], Johannes Ranft* and Paola R. Sala[#]

[#] CERN, 1211 Geneva 23, Switzerland

(on leave of absence from INFN Milan)

* Phys. Dept., Universität Siegen, D-57068 Siegen, Germany

Abstract

FLUKA is a multiparticle transport code capable of handling hadronic and electromagnetic showers up to very high energies (100 TeV), widely used for radioprotection and detector simulation studies. The physical models embedded into FLUKA are briefly described and their capabilities demonstrated against available experimental data. The complete modelling of cosmic ray showers in the earth atmosphere with FLUKA is also described, and its relevance for benchmarking the code for space-like environments discussed. Finally, the ongoing developments of the physical models of the code are presented and discussed.

1 Introduction

The beginning of the FLUKA history (see [1]) is back to 1964 when Johannes Ranft started to develop MonteCarlo codes for high energy beams, as required at CERN for many accelerator related tasks. The name FLUKA came around 1970, when first attempts were made to predict calorimeter fluctuations on an event-by-event basis (FLUKA = FLUctuating KAskades).

The present code is mostly an effort started in 1990 in order to get a suitable tool for the LHC era, and has little or no remnants of older versions. The main link with the past is Johannes Ranft, mostly in the development of the high energy generator part.

The code is in wide use at CERN and in other labs, and is *the* tool used for all radiation calculations and for the neutrino beam studies at CERN. It is the MonteCarlo of the ICARUS/ICANOE neutrino and rare event experiments, as well as it is used for the spallation part of the Energy Amplifier studies (all activities chaired by C. Rubbia).

The modern FLUKA[2, 3] is an interaction and transport MonteCarlo code able to treat all components of radiation fields within approximately the following energy ranges:

- Hadron-hadron and hadron-nucleus interactions 0-100 TeV
- Electromagnetic and μ interactions 1 keV-100 TeV
- Charged particle transport - ionization energy loss
- Neutron multigroup transport and interactions 0-20 MeV
- Analogue or biased calculations
- Nucleus-nucleus and hadron-nucleus interactions 0-10000 TeV/n: *under development, see section 6*

FLUKA can be run in fully analog mode, for calorimetry and detector response simulations. It can calculate coincidences and anticoincidences. It can also be run in biased mode, for shielding design, or for studies of deep penetration or rare events: hadron punchthrough, radiation background in underground experiments, muon production over short decay lengths.

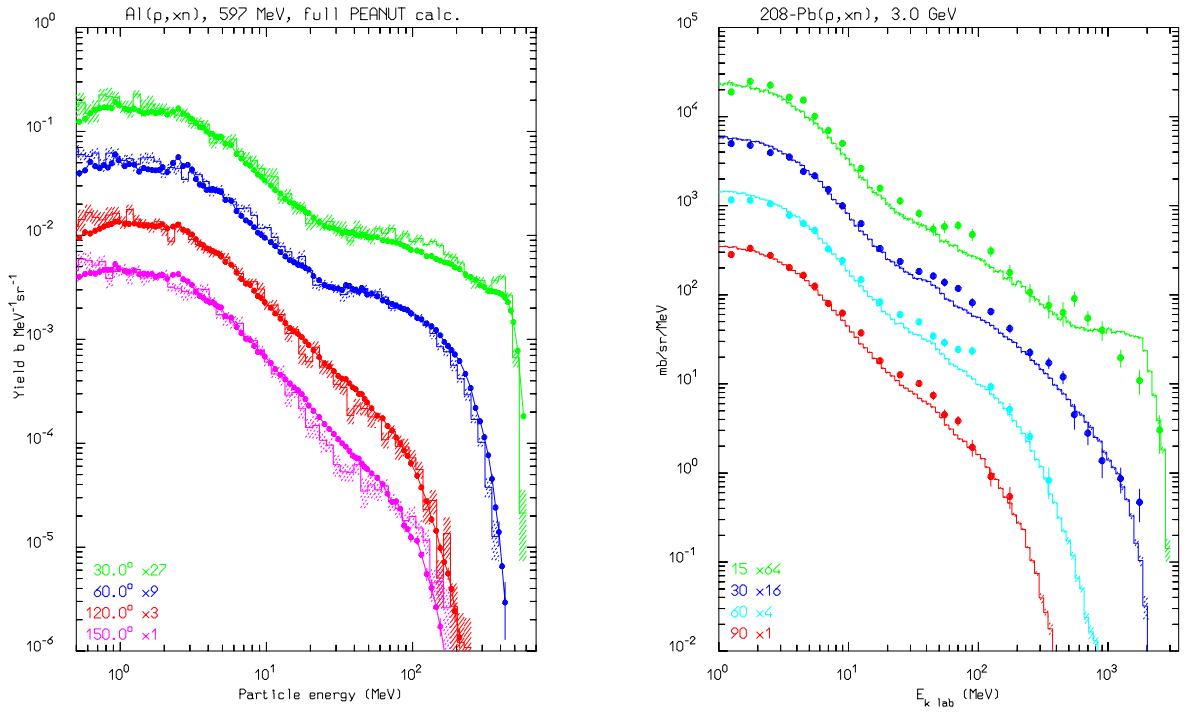


Figure 1: Computed (histograms) and experimental [6, 7] (symbols) double differential neutron distributions for Al(p,xn) at 597 MeV (left) and Pb(p,xn) at 3 GeV (right).

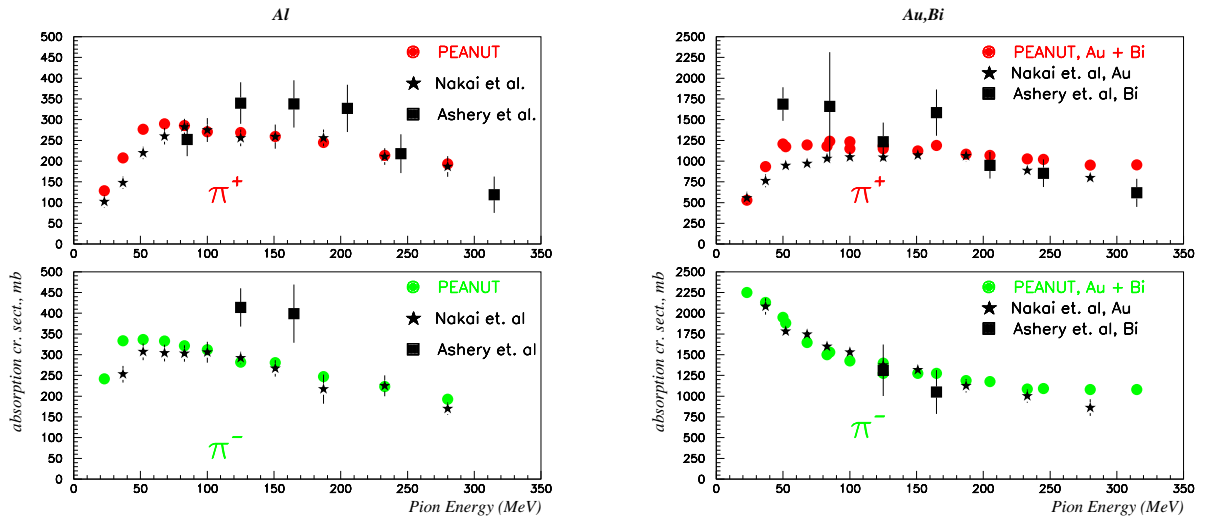


Figure 2: Computed and experimental [8] pion absorption cross section on Aluminum (left) and on Gold or Bismuth (right) as a function of energy

2 The FLUKA hadron interaction models

Two models are used inside FLUKA to describe nonelastic interactions

- The “low-intermediate” energy one, PEANUT, which covers the energy range up to 5 GeV
- The high energy one which can be used up to several tens of TeV

The nuclear physics embedded in the two models is very much the same. The main differences are a coarser nuclear description (and no preequilibrium stage) and the Gribov-Glauber

cascade for the high energy one.

In the following the description will mostly concentrate on PEANUT since it is the most relevant for space applications and it will eventually be extended to incorporate the high energy model as well. PEANUT is a three step model:

1. (Generalized) IntraNuclear Cascade
2. Preequilibrium
3. Evaporation/Fission or Fermi break-up

Hadron-nucleus non-elastic interactions are often described in the framework of the IntraNuclear Cascade (INC) models.

Classical INC codes were based on a more or less accurate treatment of hadron multiple collision processes in nuclei, the target being assumed to be a cold Fermi gas of nucleons in their potential well. The hadron-nucleon cross sections used in the calculations are free hadron-nucleon cross sections. Usually, the only quantum mechanical concept incorporated was the Pauli principle. Possible hadrons were often limited to pions and nucleons, pions being also produce or absorbed via isobar (mainly Δ_{33}) formation, decay, and capture.

Most of the historical weaknesses of INC codes have been mitigated or even completely solved in some of the most recent developments [3, 4, 5], thanks to the inclusion of a pre-equilibrium stage, and to further quantistic effects including coherence and multibody effects. Further details and validations can be found in [3]. Two examples are presented in fig.1

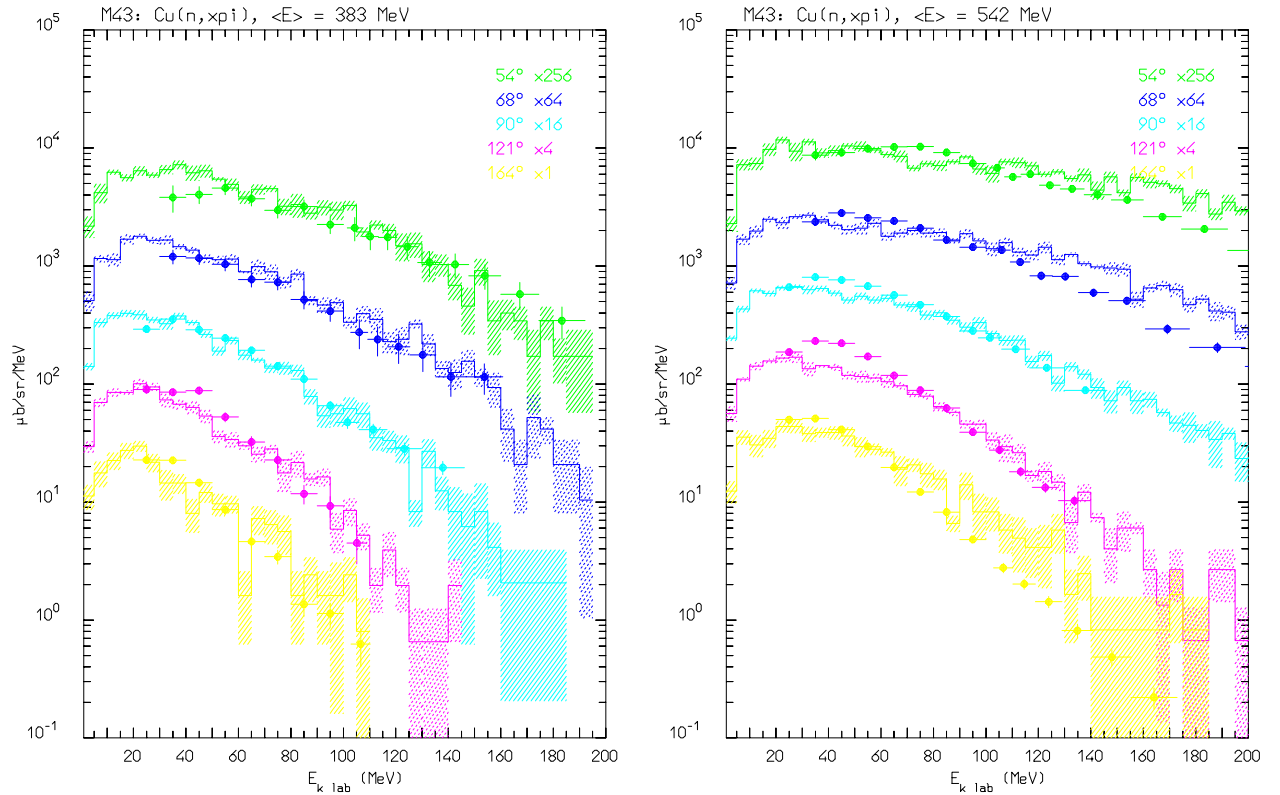


Figure 3: Double differential distributions of charged pions produced by neutrons of $\langle E_n \rangle = 383$ (left) and 542 MeV (right). Exp. data from [9]

2.0.1 Pion Interactions

An accurate description of pion production and interactions is essential in many problems involving hadronic showers, for instance in the evaluation of radiation damage. The description of pion interactions on nuclei in the sub-GeV energy range in PEANUT takes into account:

- The resonant nature of the $\pi - N$ interaction, mostly dominated by the $\Delta(1232)$.
- The effect of the nuclear medium on the $\pi - N$ interaction
- The possibility of absorption (both s-wave and p-wave) on two or more nucleons
- The resonant nature of the pion-nucleus potential, which is rapidly varying with the pion energy

The importance of the two-nucleon pion absorption, and the accuracy of PEANUT, can easily be estimated from the values in fig. 2

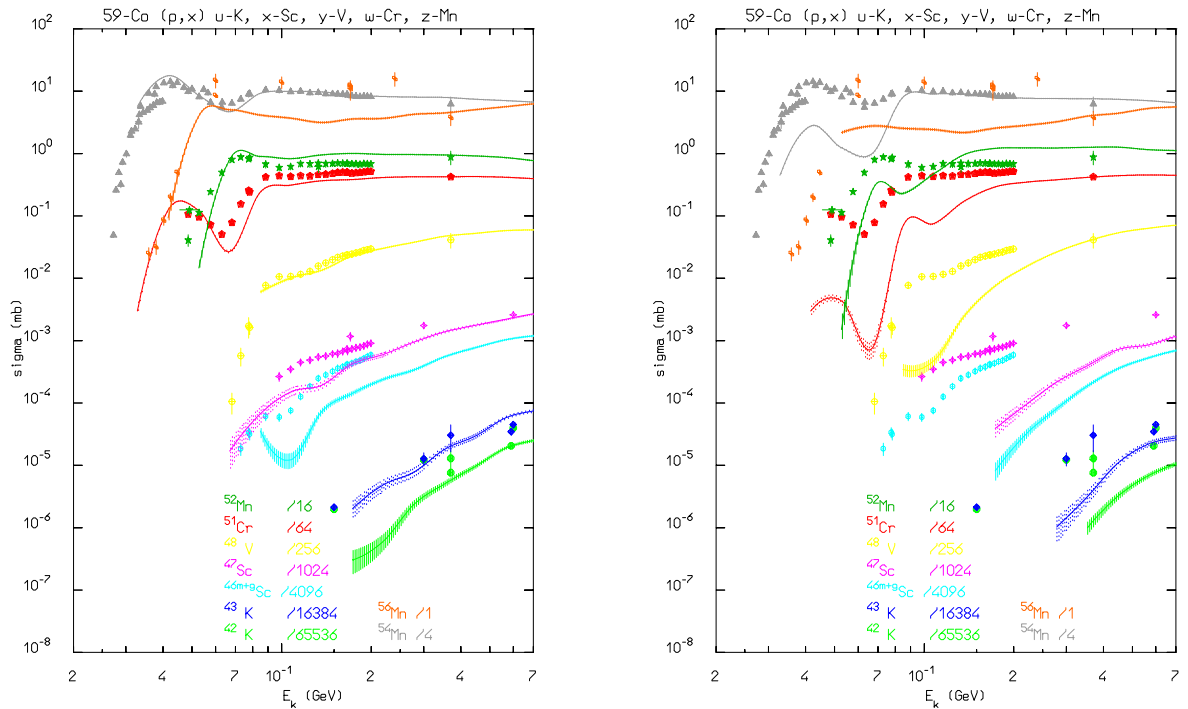


Figure 4: Comparison between isotope yields computed with the new (left) and old (right) evaporation model in FLUKA. Data from [14]

2.0.2 Single and multiple pion production

For energies in excess of few hundreds MeV the inelastic channels (pion production channels) start to play a major role. The isobar model easily accommodates multiple pion production, for example allowing the presence of more than one resonance in the intermediate state (double pion production opens already at 600 MeV in nucleon-nucleon reactions, and at about 350 MeV in pion-nucleon ones). Resonances which appear in the intermediate states can be treated as real particles, that is, they can be transported and then transformed into secondaries according to their lifetimes and decay branching ratios. Two examples are shown in fig. 3

2.1 High energy interactions

Above a few GeV a Dual Parton Model based generator is used for the description of individual hN interactions. The model includes:

- main chain diagrams for all combinations of h-h.
- Diffraction including low mass diffraction to individual resonances
- Chain hadronization with p_t and mass effects particularly tuned for (relatively) low mass quark chains

Together with the Glauber-Gribov cascade this model allows reasonable description of h-A collisions up to very high energies (details can be found in [3]). The recent developments in this model [10] made it the choice code for the Cern Neutrino to Gran Sasso simulations [11].

3 Residual nuclei predictions: the ultimate problem

Many problems require a reasonable knowledge of the identity and energy of the heavy fragments (residuals) produced in h -A and A-A interactions, both on the target and the projectile side.

The residual nuclei production is highly sensitive to the last stages of the reaction. In FLUKA, an evaporation/fission/break-up model derived from the Weisskopf-Ewing formulation is implemented. The model has been already successfully applied to h-A and A-A reactions [12, 13]. The most recent version includes:

- Level densities from Gilbert-Cameron + Ignatyuk energy dependence
- Competition with fission and γ ray emission
- Fermi Break-up for $A \leq 17$ nuclei, with optional spin-parity effects
- Sampling from emission widths without Maxwellian approximation
- Rough sub-barrier emission
- Rough spin-parity effects for low excitations

Results and improvement with respect to the old model [12] are shown in fig. 4

4 Complex benchmarks

Many complex FLUKA benchmarks about full cascade or neutron propagation can be found in the literature. Among the others: the TIARA [15] neutron propagation experiment, the TARC [16] experiment at CERN, the Röstli [17] experiments at CERN, the CERF [18] dosimetry facility at CERN, the OPTIS [19] beam at PSI (an attempt of merging biophysical and physical models).

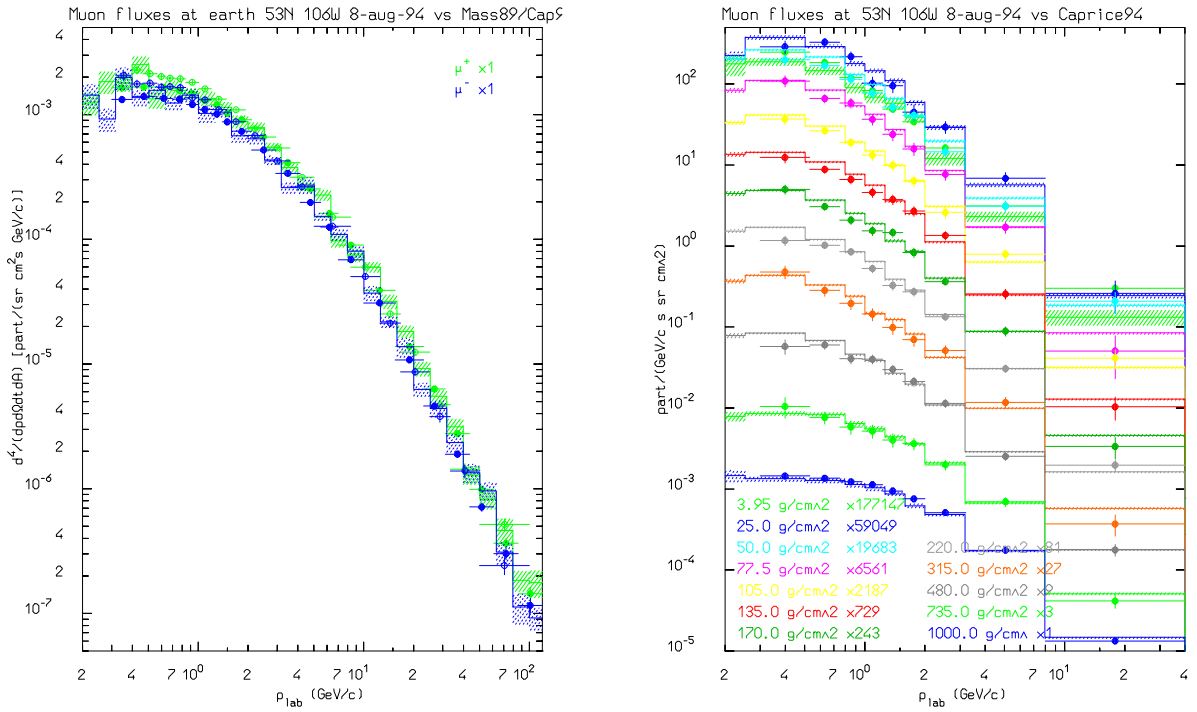


Figure 5: Muon fluxes at ground level (left) at 53N 106W on 8-aug-94 compared with data from Mass89 [20] (open symbols, 1989) and from Caprice94 [21] (full symbols). Muon fluxes at various atmospheric depths (right) on 9-aug-94, compared with Caprice94 measurements.

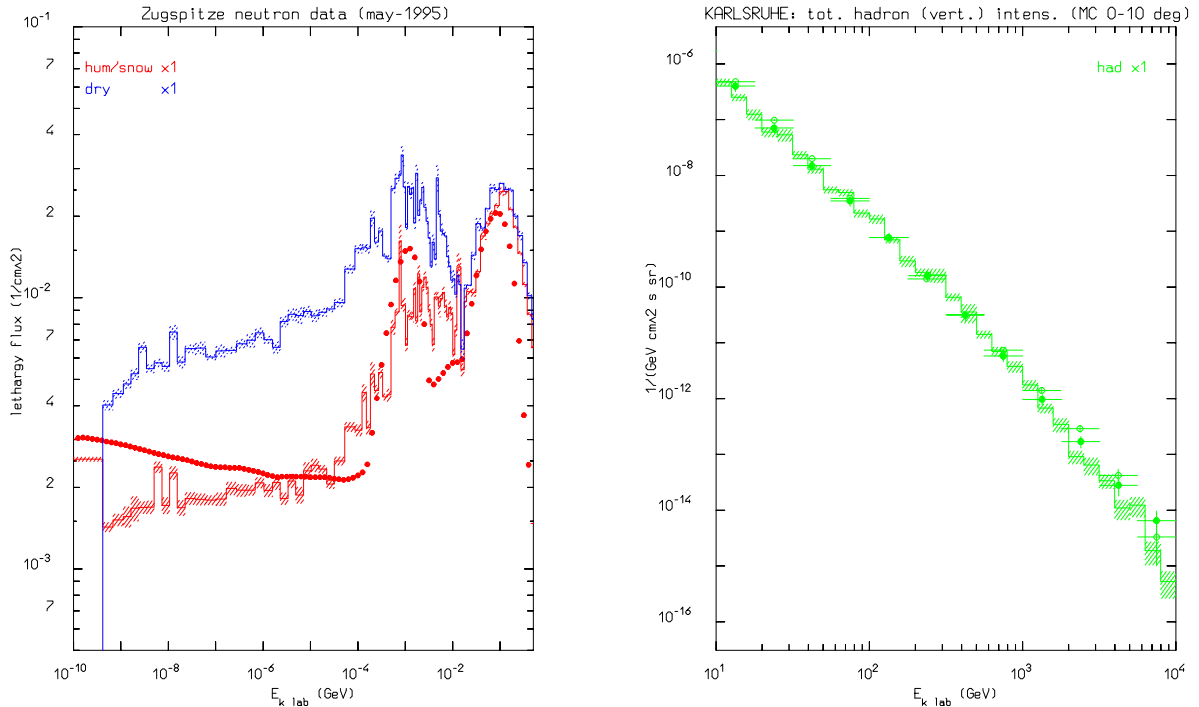


Figure 6: Neutron flux at top of the Zugspitze (left, exp. data from [22]) for dry and wet conditions, and hadron flux (right) measured with the KASKADE experiment [23].

5 From atmospheric neutrinos to aircrew doses

A new field of improvements and applications opened in the last years, driven by the goal of exploiting the FLUKA interaction models to compute atmospheric neutrino fluxes for ICARUS with unprecedented accuracy within a full 3D calculation.

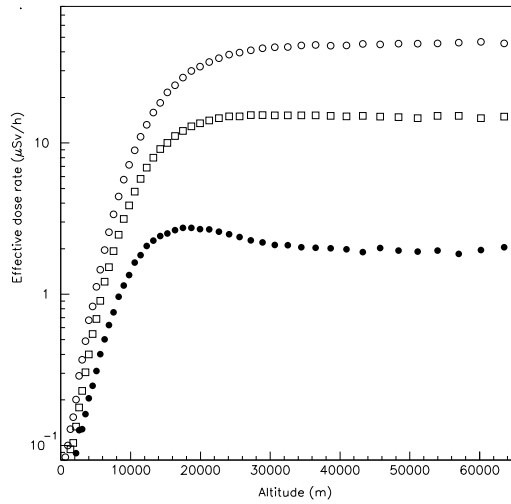


Figure 7: Calculated effective dose as a function of altitude for a vertical rigidity cutoff of 0.4 GV at solar minimum (open circles), and at solar maximum (open squares), for a cut-off of 17.6 GV (black circles)

Absorbed Dose and Dose Equivalent on Mars Surface

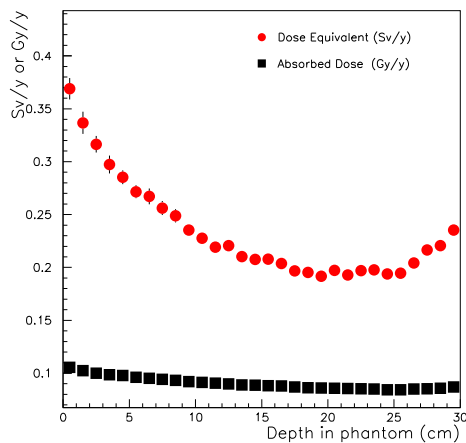


Figure 9: Computed Dose and Dose equivalent rates at Mars surface

Primary cosmic ray spectra and interplanetary modulation according to measured solar activity on a day-to-day basis have been implemented. Geomagnetic effects with full multipole expansion of the field or with a simplified offset dipole model (much faster...) have been included.

The shower simulations in atmosphere have been compared to the most recent muon and hadron spectra at different latitudes and altitudes, obtaining remarkable agreement (see figs. 5 and 6).

As a natural byproduct, FLUKA became a powerful tool for computing radiation fluxes in the earth (and Mars...) atmosphere as well as for spacecrafts or satellites.

Doses to commercial flight are the subject of a work in progress by M.Pelliccioni et al. [24],

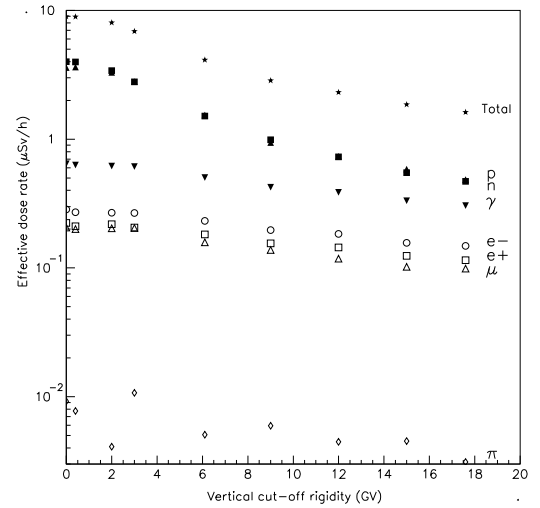


Figure 8: Contributions of various radiation components to the effective dose rate as a function of the vertical cut-off rigidity at solar minimum, for an altitude of 10580 m

Particle Fluences in Mars Atmosphere

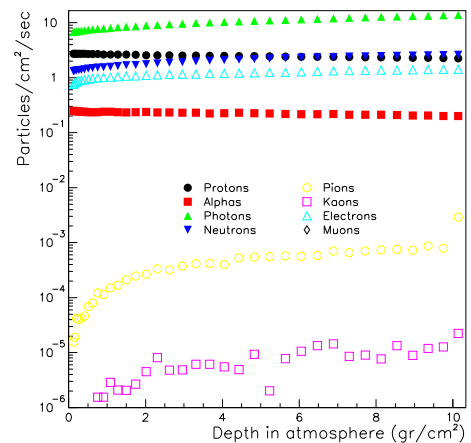


Figure 10: Particle fluences as a function of depth in the Mars atmosphere

preliminary results are shown in figs. 7 and 8.

5.1 Radiation levels at the Mars surface

A simple model of the Mars atmosphere has been setup ($\approx 10 \text{ g/cm}^2$ of CO_2), with a terrestrial rock composition for the Mars surface (*to be improved in future calculations*)

Individual energy losses have been weighted with proper factors depending on the LET, according to the most recent recommendations for quality factors issued in ICRP60, with the same procedure used in [25] when computing fluence to dose equivalent conversion data and effective quality factors for high energy neutrons.

A 30 cm thick water layer has been used as scoring phantom. For obvious statistical reasons it had to be quite large, therefore introducing a bias in the low energy neutron spectrum. Future calculations will be done in two stages

- computing the radiation environment on the Mars surface,
- simulating on a local scale a suitable phantom into such an environment.

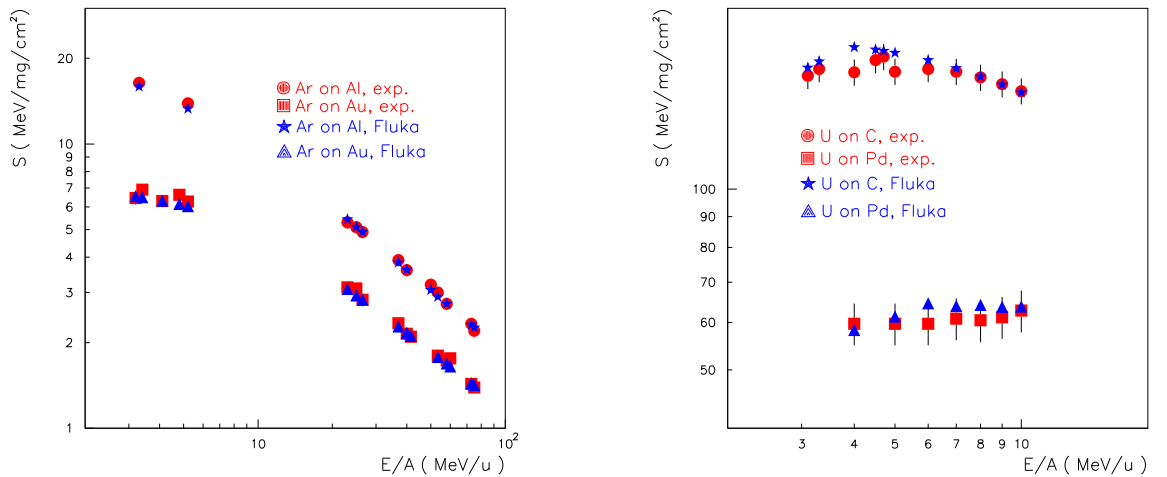


Figure 11: Comparison of experimental[26] (red) and FLUKA (blue) stopping powers of Argon and Uranium ions in different materials and at different energies.

6 Heavy ions

Heavy ion transport and interactions are presently under development in FLUKA. They are of utmost importance, for example, for dose and damage calculation in space aircrafts. Concerning ion transport (and the related LET spectra) everything has been already implemented, including up-to-date effective charge parametrization, energy loss straggling according to “normal” first Born approximation and charge exchange effects (dominant at low energies, ad-hoc model developed for FLUKA) and multiple scattering. Corrections for Mott cross section and nuclear form factors which are important for straggling at high energies are in progress.

FLUKA results about dE/dx and straggling of heavy ions are shown in fig. 11 and table 1.

High energy A-A interactions ($E > 5 - 10 \text{ GeV/n}$) will be available soon through an interface to the DPMJET code (see next section). Low energy A-A interactions will be managed by an extension of the PEANUT model. Preliminary tests with α particles are already underway.

Projectile	Target	thickness (mg/cm ²)	FWHM (keV)	
			Exp	FLUKA
¹² C	Al	0.217	74.5 ±3	90
¹⁶ O	Al	0.110	92 ±2	94
¹⁶ O	Al	0.246	147 ±3	144
¹⁶ O	Al	0.457	202 ±2	198
³² S	Al	0.315	290 ±30	356
³² S	Al	0.990	521 ±20	638
³² S	Au	0.053	98 ±20	140
³² S	Au	3.492	820 ±20	1092
¹²⁷ I	Al	0.321	780 ±40	735
¹²⁷ I	Al	0.530	1000 ±35	949
¹²⁷ I	Al	0.990	1375 ±50	1297
¹²⁷ I	Au	0.053	250 ±10	275
¹²⁷ I	Au	1.186	1200 ±50	1255
¹²⁷ I	Au	3.800	2250 ±90	1932

Table 1: Measured[27] and computed (FLUKA) straggling for 2 MeV/amu ¹²C, ¹⁶O , ³²S ions and 1.467 MeV/amu ¹²⁷I ions

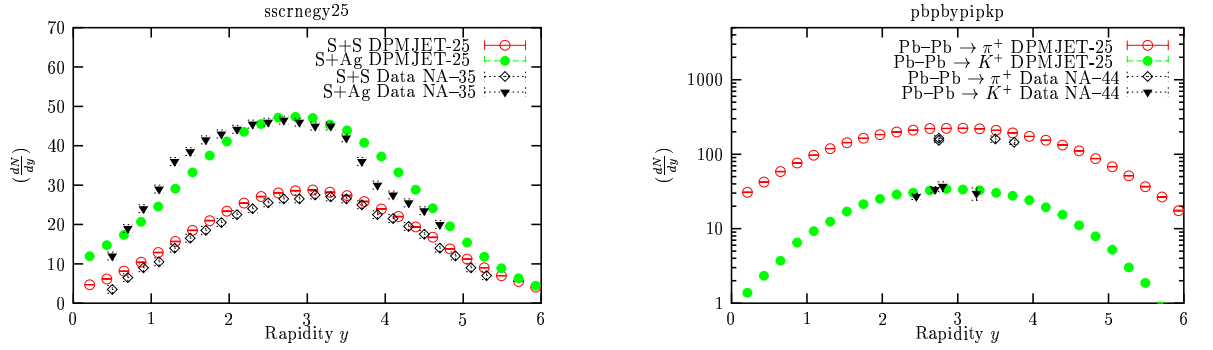


Figure 12: Rapidity distribution of negative particles for 158 AGeV/c S-S and S-Ag collisions (left) and of positive pions and kaons for 158 AGeV/c Pb-Pb collisions (right). Experimental data from the NA-35 and NA-44 collaborations are compared with DPMJET predictions.

6.1 Heavy ions at relativistic energies: DPMJET

DPMJET[28] is a Nucleus-Nucleus interaction code developed for collisions from ≈ 5 -10 GeV/n till the highest cosmic ray energies ($10^{18} - 10^{20}$ eV). The physics embedded in DPMJET has been checked against a variety of experimental data covering the range accessible to present particle accelerators.

Examples of its performances are shown in fig12. It is presently used by the ALICE at LHC experiment, and it has already been interfaced to the HEMAS-DPM code used by the MACRO Collaboration and to the CORSIKA code. Its implementation into FLUKA is under way.

7 Conclusions

The physical models embedded in FLUKA have proven to be advanced enough to provide reliable estimates of particle production and propagation in a wide range of energies and problems.

Space radiation applications will benefit from the robust physics modelling and of course from the almost unlimited capabilities in geometrical description, magnetic field transport and biasing of the code

The development of capabilities for A-A interactions comparable to those for h-A is now in progress.

Acknowledgments

The authors acknowledge the help and suggestions of M. Pelliccioni and L. Pinsky in preparing this talk.

References

- [1] J. Ranft, opening talk of the 2nd Workshop on Simulating Accelerator Radiation Environments, CERN, Geneva, october 9-11 1995, TIS-RP/97-05.
- [2] A. Fassò, A. Ferrari, J. Ranft and P.R. Sala, in Proc. of SARE-3, KEK-Tsukuba, May 7-9 1997, H. Hirayama ed., KEK report Proceedings 97-5, (1997) 32.
- [3] A. Ferrari, and P.R. Sala, Proc. of the “Workshop on Nuclear Reaction Data and Nuclear Reactors Physics, Design and Safety”, International Centre for Theoretical Physics, Miramare-Trieste, Italy, 15 April-17 May 1996, A. Gandini, G. Reffo eds, Vol. 2, (1998) 424.
- [4] S.G Mashnik and S.A. Smolyansky, JINR preprint E2-94-353, Dubna (1994).
- [5] R.E. Prael and M. Bozoian, Los Alamos report LA-UR-88-3238 (1988).
- [6] W.B. Amian et al., Nucl. Sci. Eng. **115**, (1993) 1.
- [7] K. Ishibashi et al, Nucl. Sci. Technol. **32** (1995) 827.
- [8] D. Ashery et al., **PRC23**, (1981) 2173, and K. Nakai et. al., **PRL44**, (1979) 1446.
- [9] Buchle et al. **NPA515**, (1990) 541.
- [10] G. Collazuol, A. Ferrari, A. Guglielmi, and P.R. Sala, **NIMA449**, (2000) 609.
- [11] R. Baldy et al., Addendum to report CERN 98-02, INFN/AE-98/05, CERN SL-99-034 DI and INFN/AE-99/05 (1999).
- [12] A. Ferrari, P.R. Sala, J. Ranft, and S. Roesler, **ZPC70**, (1996) 413.
- [13] A. Ferrari, P.R. Sala, J. Ranft, and S. Roesler, **ZPC71**, (1996) 75.
- [14] A.S. Iljinov et al., Landolt-Börnstein, **Vol. 13a** (1991).
- [15] Y. Nakane et al., Proc. of the SATIF-3 workshop, Sendai, Japan, 12-13 may 1997, edited by OECD/NEA, Paris (1998), 151.

- [16] H. Arnould et al., **PLB458** (1999) 167.
- [17] A. Fassò, A. Ferrari, J. Ranft, P. R. Sala, G. R. Stevenson and J. M. Zazula, **NIMA332**, (1993) 459.
- [18] A. Esposito et al, Rad. Prot. Dos. **76**, (1998) 135.
- [19] M. Biaggi et al., **NIMB159**, (199) 89.
- [20] R. Bellotti et al., **PRD53**, (1996) 35.
- [21] M. Boezio et al., **PRL82**, 4757 (1999).
- [22] H. Schraube et al., Radiat. Prot. Dos. **70**, (1997), 405.
- [23] H.H Mielke et al. **JPG20**, (1994) 637, H. Kornmayer et al, **JPG21**, (1995) 439.
- [24] A. Ferrari, M. Pelliccioni and T. Rancati, “Calculation of the radiation environment caused by galactic cosmic rays for determining air crew exposure” submitted to Radiat. Prot. Dos.
- [25] A. Ferrari, and M. Pelliccioni, Radiat. Prot. Dos. **76**, 215 (1998).
- [26] R.Bimbot, **NIMB69** (1992) 1.
- [27] S. Ouichaoui et al. **NIMB164** (2000) 259.
- [28] J. Ranft, **PRD51** (1995) 64; Gran Sasso INFN/AE-97/45 (1997); hep-ph/9911232; hep-ph/9911213; hep-ph/0002137.